Colloid-colloid hydrodynamic interaction around a bend in a quasi-one-dimensional channel

Emily Liepold, Ryan Zarcone, and Tibor Heumann
James Franck Institute, University of Chicago, Chicago, Illinois 60637, USA

Stuart A. Rice*
The James Franck Institute and Department of Chemistry, The University of Chicago, Chicago, Illinois 60637, USA

Binhua Lin†
The James Franck Institute and Center for Advanced Radiation Sources, The University of Chicago, Chicago, Illinois 60637, USA
(Received 18 November 2016; revised manuscript received 26 January 2017; published 24 July 2017)

We report a study of how a bend in a quasi-one-dimensional (q1D) channel containing a colloid suspension at equilibrium that exhibits single-file particle motion affects the hydrodynamic coupling between colloid particles. We observe both structural and dynamical responses as the bend angle becomes more acute. The structural response is an increasing depletion of particles in the vicinity of the bend and an increase in the nearest-neighbor separation in the pair correlation function for particles on opposite sides of the bend. The dynamical response monitored by the change in the self-diffusion $[D_{11}(x)]$ and coupling $[D_{12}(x)]$ terms of the pair diffusion tensor reveals that the pair separation dependence of D_{12} mimics that of the pair correlation function just as in a straight q1D channel. We show that the observed behavior is a consequence of the boundary conditions imposed on the q1D channel: both the single-file motion and the hydrodynamic flow must follow the channel around the bend.

DOI: 10.1103/PhysRevE.96.012606

I. INTRODUCTION

The confinement of a colloid suspension to a quasi-one-dimensional (q1D) channel generates a correlation between the colloid particle motions. This correlation arises from two sources: (i) the single-file motion associated with the nonzero size of a particle and its near filling of the channel width and (ii) the hydrodynamic interaction that arises from the motion of one particle which creates a carrier fluid flow that affects the velocities of other nearby particles. That flow must satisfy the boundary conditions imposed by the q1D confinement. Unlike the three-dimensional unbounded case for which the colloid-colloid hydrodynamic interaction falls off as the inverse of the separation between the particles [1], the boundary condition imposed by the walls of a straight q1D channel leads to exponential screening of the hydrodynamic interaction on a length scale determined by the width of the channel. One consequence of this screening is that only nearest-neighbor and next-nearest-neighbor hydrodynamic interactions play a prominent role in the q1D diffusive dynamics.

Hydrodynamic coupling between particles in a q1D colloid suspension can be monitored by measurement of the separation dependences of the components of the pair diffusion tensor, $D_{ij} \equiv \langle \Delta x_i \Delta x_j \rangle / 2t$; D_{12} characterizes the effect of the motion of particle 1 on the motion of particle 2. Cui *et al.* have reported measurements of D_{12} in a straight q1D suspension along with a hydrodynamic analysis for the limiting case that the colloid particle radius is small relative to both the channel width and the mean spacing between particles, and the particle motion is restricted to be along the axis of the channel [2]. Their analysis accurately accounts for the general features of the separation dependence of D_{12} for separations greater than several particle diameters but cannot account for the small separation dependence of D_{12}. In the small separation regime the nonzero size of the colloid particles must be accounted for, as is done in the Xu *et al.* analysis of the influence of hydrodynamic coupling between a pair of particles on D_{12} and on the self-diffusion coefficient (D_{11}) in a straight q1D system [3]. Arguably the most important qualitative feature of their predictions is that the functional forms of D_{11} and D_{12} are dominated by and mimic the separation dependence of the pair correlation function of the q1D colloid suspension. The extant theory describing the influence of the excluded volume and hydrodynamic interactions in a q1D channel on the density dependence of the one-particle diffusion coefficient and the separation dependence of the relative pair diffusion coefficient are in very good agreement with experimental data [4,5].

The motivation for the study reported in this paper is the observation that in the conventional analysis of colloid-colloid hydrodynamic interaction the excess pressure generated by the Brownian displacement of one particle on a distant particle can be treated as a macroscopic fluid flow problem. With that observation in mind we note that when a fluid in a channel is forced to flow around a bend, because of centrifugal acceleration due to the channel curvature, a secondary flow is generated; the secondary flow velocity lies in planes perpendicular to the primary direction of motion [6,7]. Although that secondary flow is very weak for the typical fluid velocity induced by the Brownian particle displacement, it can in principle affect the separation dependence of the particle-particle hydrodynamic coupling. Entropic "excluded-volume" effects have also been shown to affect the motion of colloids in aqueous suspension on curved silicon substrates [8,9]. In principle, the curvature of our bent q1D channels could similarly affect the equilibrium structure of the colloids in the fluid.

In the following text we report the results of an experimental study of how the introduction of a bend in a q1D channel affects

*Corresponding author: sarice@uchicago.edu
†Corresponding author: lin@cars.uchicago.edu

the interaction between colloid particles that are on opposite sides of the bend. We note that the boundary conditions require that in a bent channel distances between particles be measured along the centerline of the channel because (i) the hydrodynamic coupling of the particles is via fluid flow around the bend and (ii) the walls of the channel force the particle trajectories and the excluded volume interaction to follow the channel. Thus, the measure of distance between particles on opposite sides of the bend follows the centerline around the bend. Using that coordinate system our experimental data show that the introduction of a bend in a q1D channel leads to changes in the one-particle and pair distribution functions of the colloid suspension as the bend is traversed. We also report the results of Monte Carlo simulations of the single and pair correlation functions of hard disks constrained to move on a 1D path with a bend with radius of curvature comparable to the disk diameter which reproduce these features of the one-particle and pair distribution functions. Using D_{12} as a monitor of hydrodynamic correlations between colloid particles our experimental data show that the separation dependence of D_{12} mimics the behavior of the pair correlation function, just as in a straight q1D channel. Thus, under equilibrium conditions, in the absence of macroscopic flow, the hydrodynamic component of the colloid-colloid interaction is affected by the bend in the q1D channel only via the structural changes in the paircorrelation function associated with the bend.

II. EXPERIMENTAL PROCEDURE

A. Apparatus

Our experimental system consists of several extended channels, each with a bend between two straight arms. The channels are filled as described below with an aqueous suspension of spherical silica particles that are restricted to diffuse along the channel. Two types of channel bends were fabricated: smooth and sharp. Smooth bends connect two straight channels with a small angular sector that preserves the width of the channel, whereas sharp bends are formed from the intersection of two straight channels. Whereas single-file motion is enforced everywhere in a channel with a smooth bend, in a channel with a sharp bend particles can pass one another at the apex of the bend. Snapshots of experimental 3 μm channels with smooth and sharp bends are displayed in Fig. 1, and schematics of both geometries are shown in Figs. 1(c) and 1(d).

Our experimental cell consists of a polydimethylsiloxane (PDMS, Sylgard 184) substrate with grooved channels along its surface. The PDMS cell is prepared by pouring uncured PDMS over a silicon wafer that has been lithographically etched with a negative of the desired design. The channels, with length $L = 2$ mm, have a depth of $d = (3.0 \pm 0.2)$ μm and bends of 60°, 90°, and 120°; data for straight (180°) q1D channels are obtained from the straight arms of any of the channels. The colloids used in our experiments are silica spheres (Duke Standards 8150), with a mass density of 2.2 g cm^{-3} and a diameter $\sigma = 1.57(2)$ μm. The parent sphere suspension was diluted with deionized water to have a colloid volume fraction of 0.1%–1.0%. Approximately 30 μL of the diluted solution was deposited onto the experimental cell containing the channel patterns. Four 100-μm-thick glass spacers were placed around the sample and a thin glass coverslip was placed on top of the spacers to prevent the sample from drying. We note that the channels are filled from the supernatant suspension by sedimentation. This method of preparation does not permit direct control of the density

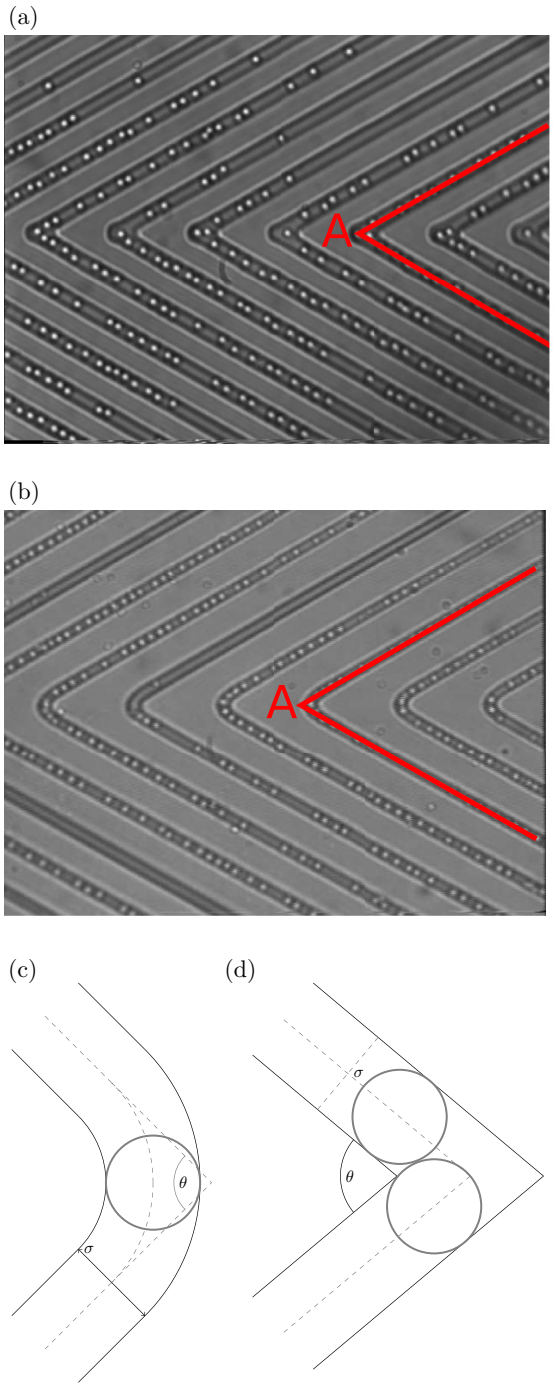

FIG. 1. Snapshots of (a) a 3 μm q1D channel with a 60° sharp bend and (b) a 3 μm q1D channel with a 60° smooth bend. The bend apices are marked with a red "A" and the centerline coordinate x is marked in red. These geometries are approximated by the geometry shown in (c) and (d) for smooth and sharp bends, respectively.

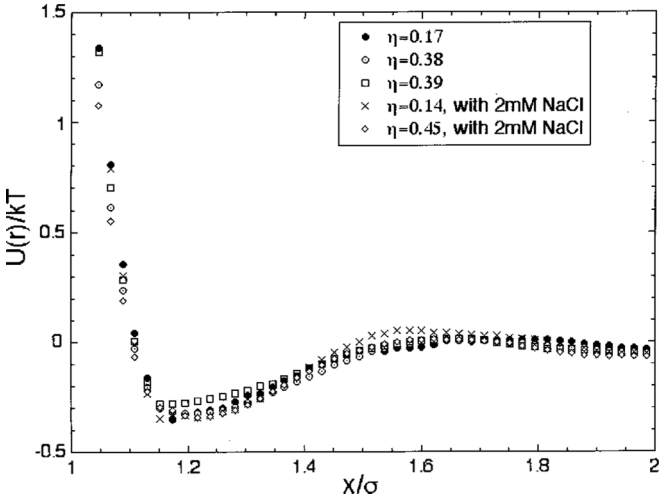

FIG. 2. The measured pair potentials between 1.58 μm colloids in 3.0 μm channels. This figure is reproduced with permission from Fig. 8 of [10].

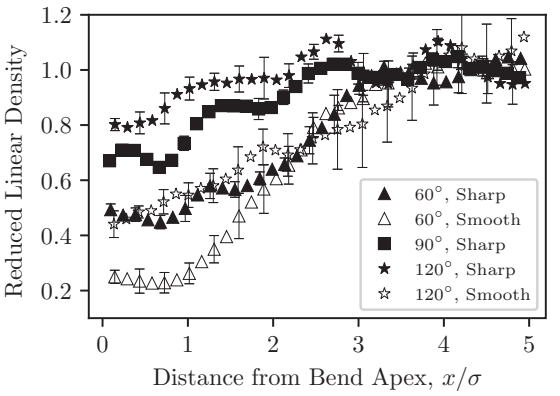

FIG. 3. Linear particle density as a function of distance from the apex of the bend in q1D channels. The density values have been reduced by dividing by the mean density ($\eta = 0.6$).

of colloids in a channel. Rather, the density of colloids in a channel is determined from the microscope images and particular samples with desired packing fraction, $\eta = N\sigma/L$, are chosen for detailed examination. The depth of the channels confines the particles with a gravitational potential of about $14k_bT$ and our microscope images show that the particles remain closely restricted to the focal plane, fluctuating out of that plane by less than 0.2σ.

The effective colloid-colloid interaction was determined in earlier work in this laboratory, from experiments with the same colloid particles in similar PDMS cells and in suspensions with different ionic strengths. The calculation of the interaction accounted for the polydispersity of the colloids and the optical anomalies arising from incipient image overlap. The inferred particle-particle pair potential consists of a strongly increasing short-ranged repulsion for separations less than $x \equiv r/\sigma = 1.1$, followed by a very weak attractive well of about $0.3k_bT$ at a separation of about $x = 1.2$ [10]. This pair potential is plotted in Fig. 2. For the range of separations probed in our experiments the colloid-colloid interaction is adequately approximated as a short-ranged near hard sphere repulsion. Charge-charge interactions were found to have negligible effect on the potential.

We prepared smooth and sharp cornered channels with (3.0 ± 0.2) μm width. However, we focus attention on measurements taken in the smooth channel because particle motion is constrained to be single file everywhere. We use measurements taken in the 3 μm channels with sharp bend to emphasize some points of our argument.

B. Data analysis

Our data were collected with an Olympus BH2 metallurgical microscope with a 100× oil-immersion objective and 2.5× video eyepiece. Images were recorded at 30 frames per second and then digitized for analysis. Particles were detected and tracked in the digitized images, using the Crocker-Grier algorithm [11], to produce short duration (0.2 s) trajectories. The particle displacements parallel to and perpendicular to the centerline of the channel were recorded. The colloid motion is more tightly constrained ($< \pm 0.1\sigma$) to the channel axis than expected from the geometric ratio of particle diameter to channel width [10]. It has been shown that in q1D systems the diffusion parallel to the channel centerline is independent of the position perpendicular to the centerline [12]. As already mentioned, particle positions were measured along the centerline of the channel; a particle at $x = 0$ is at the apex of the bend and x denotes the distance from the apex along the centerline, shown as a dashed line in Figs. 1(c) and 1(d).

C. Simulation procedure

Monte Carlo simulations of assemblies of hard disks with diameter σ, whose centers are constrained to move on a line with a bend mimicking the channel geometry, were carried out to help interpret the experimental findings. Simulations were carried out for arrays of disks on lines with bends between 45° and 180°, for linear packing fractions between 0.4 and 0.9, and for radii of curvature of the bend of σ and 0.1σ, with the latter representing a channel formed by the intersection of two straight channels. In each step of our simulations the hard disks were displaced from their previous positions by randomly chosen distances selected from a Gaussian distribution with width 0.01σ. Simulation steps that generated overlaps of disks were rejected and new steps successively selected until one that satisfied the no-overlap criterion was found. This process was repeated for $\sim 10^9$ steps to ensure that the system reached equilibrium.

III. EXPERIMENTAL RESULTS

A. Linear density profiles

Time-averaged linear density profiles were calculated from the experimental data by dividing the channel axis into bins with width 0.1σ and averaging the number of particles in each bin over all frames along the trajectory. The displacements parallel to the centerline of the channel of particles whose centers deviate from the centerline were obtained from projections onto the centerline. The resulting distributions for several suspensions with packing fraction $\eta = 0.6$ in q1D channels with different bend angles are displayed in Fig. 3. We

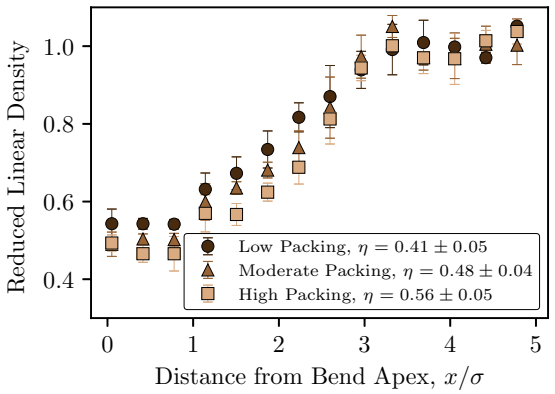

FIG. 4. Linear density as a function of distance from the apex of the bend in a 60° q1D channel. The density values have been reduced by dividing by the mean density.

find that there is a pronounced depletion of the linear density in the region around the apex of the bend (Fig. 4). The data displayed show that the magnitude of the density depletion increases as the bend angle becomes more acute. Figure 3 also shows that the depletion is smaller, for a given bend angle, in a 3 μm channel with a sharp bend than in a 3 μm channel with a smooth bend, which we attribute to the violation of the single-file ordering in the sharp corner channel.

B. Pair distribution functions

Given the behavior of the linear density distribution in the domain including the bend in the channel we expect the pair distribution functions for particles separated by the bend to differ from that when both particles are in a straight portion of the channel. We show in Fig. 5(b) the pair distribution functions for particles on opposite sides of the bend in 60° and 120° channels along with that for the straight q1D channel; in the 60° channel there is a very significant increase of the nearest-neighbor separation relative to that in the straight portion of the channel. As shown in Fig. 6, there is a monotone increase in the nearest-neighbor separation of the opposite side pair correlation function as the bend angle is made more acute; these observations are independent of the smooth or sharp nature of the bend and very weakly dependent on the average packing fraction (Fig. 7). The 120° and 180° data displayed in Fig. 5(b) show the pair correlation function decreasing rapidly in the domain $0 < r/\sigma < 1.3$ as $r/\sigma \to 0$, whereas the 60° data show the pair correlation function decreasing slowly in that domain as $r/\sigma \to 0$. The shape of the 60° data is an anomaly resulting from the use of distance along the centerline of the channel to monitor particle-particle separation, since the relationship between centerline separation and center-to-center geometric separation is not a linear function of the bend angle. Indeed, the same unusual decay of the pair correlation function is found from the Monte Carlo simulations reported in Sec. III C.

C. Monte Carlo simulation results

The results of our Monte Carlo simulations reproduce the major features of the single particle and pair distribution

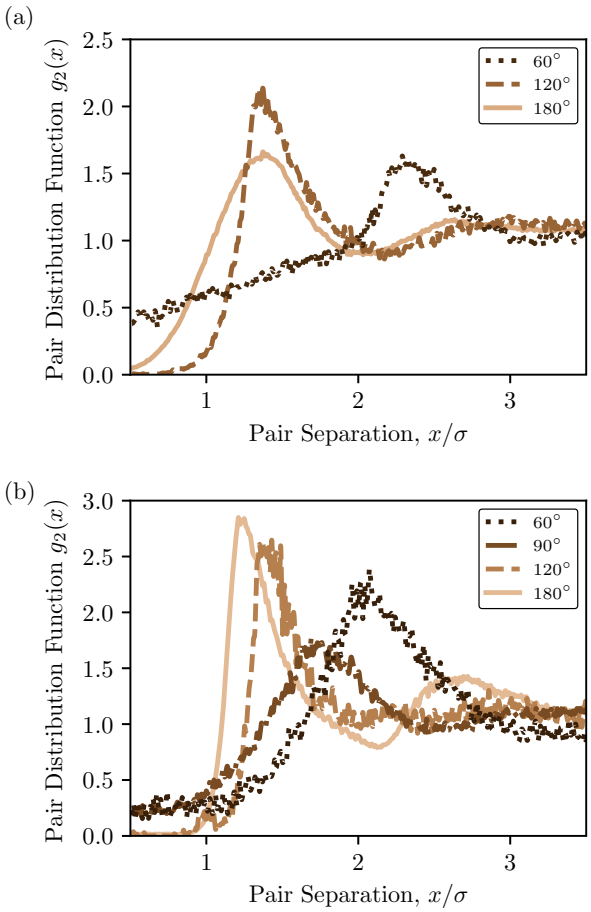

FIG. 5. Pair distribution functions for particles on the same side (180°) and on opposite sides of acute bends in smooth (a) and sharp (b) 3 μm q1D channels.

functions reported in the last section. We show in Fig. 8 the pair distribution functions obtained from the simulations for suspensions in q1D channels with bend angles 60°, 75°, 150°, and 180°. These should be compared with the experimental data for the 3 μm smoothly bent channels because of the

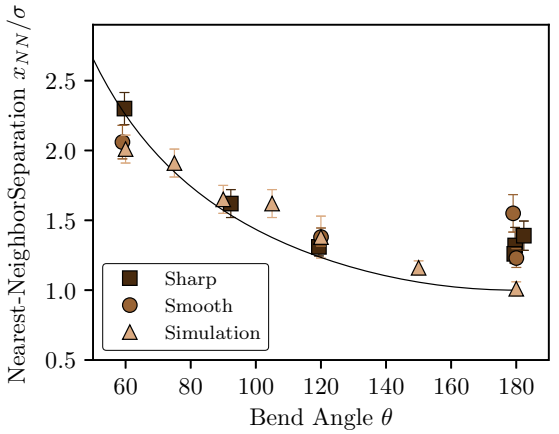

FIG. 6. Separation of nearest-neighbor particles on opposite sides of the bend in a 3 μm q1D channel as a function of the bend angle for a suspension with $\eta = 0.6$. The solid line is a plot of Eq. (7).

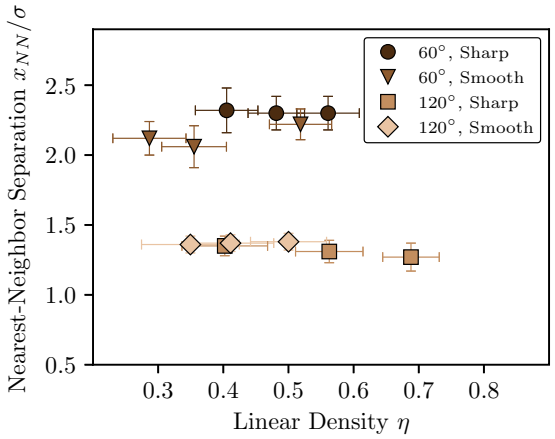

FIG. 7. Position of the first peak of the pair correlation function for particles on opposite sides of the bend in 60° and 120° q1D channels as a function of packing fraction.

constraint in the Monte Carlo simulations that the particle centers must be displaced along the line.

D. Pair diffusion coefficient measurements

As already mentioned, we monitor the effect of the hydrodynamic coupling between colloid particles via determination of the pair diffusion tensor with elements D_{ij} [13],

$$D_{ij} = \frac{\langle \Delta x_i \Delta x_j \rangle}{2t}. \tag{1}$$

The D_{ij} measure the self- and distinct correlations between the displacements of particles i and j in time t. In our q1D geometry $D_{11} = D_{22}$ is the self-diffusion coefficient of a particle in the presence of another particle at a distance r, averaged over the positions of all other particles in the system, and D_{12} characterizes the effect of the motion of particle 1 on the motion of particle 2 at a distance r, averaged over the positions of all other particles in the system. The experimental trajectories can be analyzed to yield both the center-of-mass (D^+) and relative (D^-) pair diffusion coefficients defined by

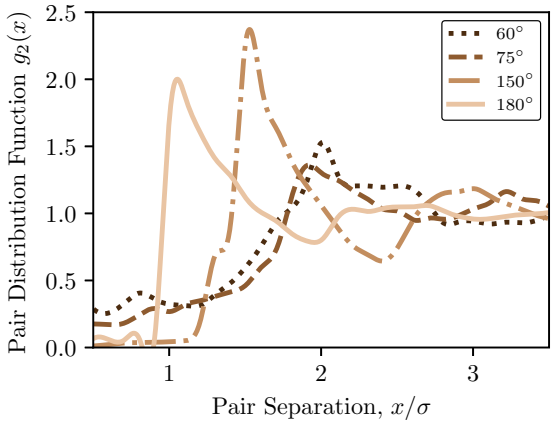

FIG. 8. Pair distribution functions obtained from Monte Carlo simulations for suspensions in q1D channels with bend angles 60°, 75°, 150°, and 180°.

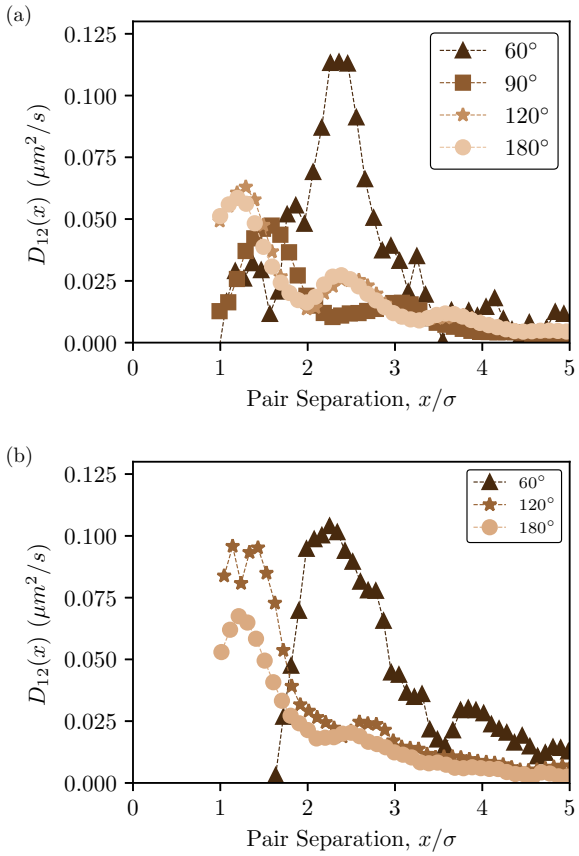

FIG. 9. Dependence of $D_{12}(x)$ on the pair separation for particles on opposite sides of the bend in channels with (a) sharp and (b) smooth bends.

$$D^{\pm} = \frac{\langle [\Delta x_2(t)]^2 + [\Delta x_1(t)]^2 \pm 2\Delta x_2(t)\Delta x_1(t) \rangle}{4t} \tag{2}$$

$$= \frac{D_{11} \pm D_{12}}{2}. \tag{3}$$

We will focus attention on the separation dependence of the relative pair diffusion coefficient

$$D_{12}(x) = \frac{D^+(x) - D^-(x)}{2}. \tag{4}$$

We calculated $D_{12}(x)$ for all pairs of particles separated by $x \pm \frac{1}{2}dx$ with $dx = 0.11\sigma$, both for pairs of particles on the same side of the bend and for pairs of particles on opposite sides of the bend in the q1D channel. We required members of "same side" pairs to both be more than 5σ from the bend apex to minimize any influence from the bend. The time intervals used for measuring D_{12} were small (< 1.0 s), less than the crossover time between the diffusive and subdiffusive regimes of q1D motion [14,15]. The dependences of $D_{12}(x)$ on bend angle for particles on opposite sides of the bend in the 3 μm sharp and smooth bend channels are shown in Figs. 9(a) and 9(b), respectively. The separation at which the peak in $D_{12}(x)$ occurs is the same for channels with the smooth and sharp bends, and is sensibly independent of packing fraction (Fig. 10). The pair separation at which the peak in $D_{12}(x)$ appears decreases monotonically as the bend angle decreases (Fig. 11), just as

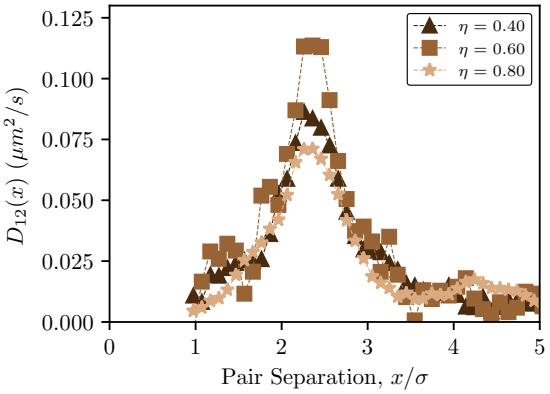

FIG. 10. Dependence of $D_{12}(x)$ on x in the 60° channel, for several packing fractions.

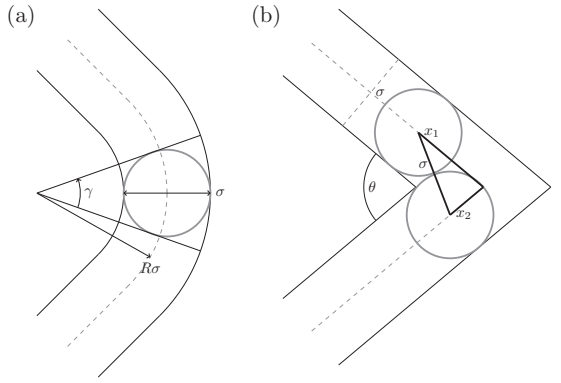

FIG. 12. Diagrams demonstrating the sharp and smooth bend geometries.

does the nearest-neighbor separation (Fig. 6) exhibited by the pair correlation function. To emphasize their similarity, both quantities—nearest-neighbor separation calculated from $g_2(x)$ and the peak in $D_{12}(x)$—are plotted together in Fig. 11.

IV. DISCUSSION

The results described in the preceding sections show that the (i) local packing of colloid particles in a suspension in the smooth bend region of a bent q1D channel differs from that in a straight q1D channel and (ii) that the hydrodynamic component of the colloid-colloid interaction is affected by the bend in the q1D channel only via changes in the pair correlation function associated with the bend. In particular, the particle separation dependence of $D_{12}(x)$ mimics the behavior of the paircorrelation function, just as in a straight q1D channel.

We examine first the linear density deficiency in the apex region of the bent q1D channel. The geometry of the smoothly bent channel is sketched in Fig. 12(a). We consider the case that the channel has width σ equal to the particle diameter, and that the bend in the channel, with radius of curvature of the centerline equal to $R\sigma$, preserves the channel width. If a particle is centered in the apex of the bend it subtends an angle $\gamma = 2\arctan(4R^2 - 1)^{-1/2}$. In a linear close-packed array in the straight portion of the channel the fraction of space occupied by a disk is $\eta = \frac{\pi\sigma^2}{4\sigma^2}$, whereas a particle located at the apex of the bend occupies a fraction of the annular space [Fig. 12(a)] equal to $\eta = \frac{\pi}{4R\gamma}$. We note that in this construction the radius of curvature is restricted to $R \geqslant 1/2$ and that for a radius of curvature comparable to the particle radius the packing fraction per particle is less than that in the straight channel: $\eta(R = 0.50) = 0.50$, $\eta(R = 0.75) = 0.717$, and $\eta(R = 1.0) = 0.75$ (see Fig. 13). The radius of curvature of the smooth channel we have used in our experiments is not known with precision but a visual inspection suggests that it is comparable to the particle radius. The observed single particle density depletion in the bend angle region is qualitatively similar to that predicted from the idealized simple model described above, but larger in magnitude. We suggest that this difference is a consequence of the difference between the model channel and the real channels. In the experimental realizations of the bent channels the ratio of particle diameter to channel width is, although large enough to enforce single-file motion, less than one, thereby allowing more space per particle than assumed to be the case in the model channel.

Our experiments show that the dependence of the nearest-neighbor separation for particles on opposite sides of the bend

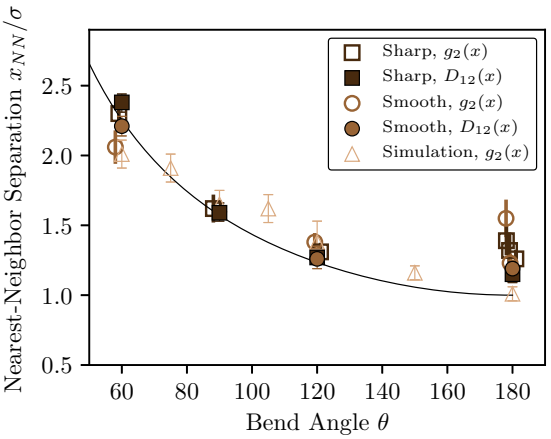

FIG. 11. Comparison of the locations of the first neighbor separation obtained from $g_2(x)$, the peak in $D_{12}(x)$, and Eq. (7) (solid line).

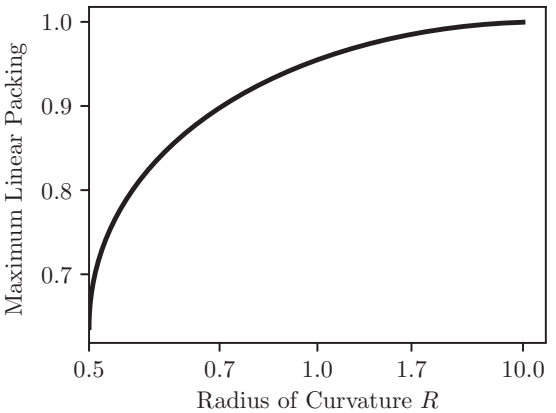

FIG. 13. Packing fraction around a particle located at the apex of the bend in a smooth channel with width σ and centerline radius of curvature $R\sigma$.

in the channel, measured along the centerline of the channel, is the same for smooth and sharp bends (Fig. 6). We now argue that the form of the observed dependence is a consequence of measuring the particle-particle separation along the centerline rather than directly along the line of centers. Consider a channel with width equal to a particle diameter and a sharp bend. Let two particles that are in contact be at distances x_1 and x_2 from the apex of the bend, measured along the centerlines of the two arms of the channel. This configuration is shown in Fig. 11(b). The separation of the particles, $s(\theta) = x_1 + x_2$, clearly depends on θ, and the line connecting the centers of the particles does not lie along the centerline of the channel. Setting $\sigma = 1$, and using the constraint that the two particles are in contact, we have

$$[x_2\cos(\theta/2) - x_1\cos(\theta/2)]^2 + [x_2\sin(\theta/2) + x_1\sin(\theta/2)]^2 = 1. \quad (5)$$

With $x_1 \leqslant x_2$ and $\lambda = \cos^2(\theta/2)$ Eq. (5) has a solution that reads

$$s(x_1,\lambda) = 2x_1\lambda + \left[1 - 4x_1^2(\lambda - \lambda^2)\right]^{1/2}. \quad (6)$$

We note that a particle lies entirely on one side of the apex of the bend when $x_1 = x' = [2\sin(\theta/2)] = 2\sqrt{1-\lambda}$, beyond which point the particles no longer are in contact. The dependence of $s(x_1,\lambda)$ on x_1 can be removed by averaging $s(x_1,\lambda)$ with respect to the allowed values of x_1. This average is

$$\langle s(\lambda)\rangle = \frac{1}{x'}\int_0^{x'} dx_1 s(x_1,\lambda) = \frac{\lambda}{\sqrt{1-\lambda}} + \frac{\sqrt{1-\lambda}}{2} + \frac{\sin^{-1}[(1-\lambda)\sqrt{\lambda}]}{2(1-\lambda)\sqrt{\lambda}}. \quad (7)$$

Equation (7) is plotted, as a function of the bend angle of the channel, in Figs. 6 and 11. Clearly, the apparent shift in the first peak of the pair correlation function is associated with the change in coordinates used to describe the particle-particle separation that is enforced by the boundary conditions. That is, because the boundary conditions determine the path followed by both the solvent and the particles as they travel through the bend, the path followed along the centerline is longer than the center-center path, and we can consider the choice of the coordinates along the channel centerline to be a dilation of the length scale of the problem. Accordingly, we observe both a decrease of the linear density and an increase in the nearest-neighbor length scale in traversing the bend in the q1D channel.

We consider now the hydrodynamic contribution to the components of the pair diffusion tensor. As already noted, the hydrodynamic interaction between particles in a q1D channel is screened on the scale length of the channel width. Consequently, particles move in concert only when their separation is smaller than the channel width and two body interactions remain dominant up to high particle density. The center of mass and relative diffusion coefficients of a pair of particles approach the sum of the single particle diffusion coefficients at large particle separation. However, at small particle separation the center-of-mass diffusion coefficient exceeds, and the relative diffusion coefficient is less than, the sum of the single particle diffusion coefficients. To account for separation dependencies of $D_{11}(x)$ and $D_{12}(x)$ it is necessary to account for the nonzero size of the colloid particles and the effect of one particle on the flow near the other and near the walls of the channel. The analysis of the hydrodynamic coupling in a suspension confined to a q1D channel reported by Xu *et al.* goes beyond the Stokeslet approximation by using the so-called method of reflections and an average over all possible configurations of the particles; it properly accounts for the nonzero size of the colloid particle [3]. Like the Stokeslet analysis, it exploits the fact that when the particle velocity is very small the hydrodynamic interactions between particles and between each particle and the wall can be described by the linear Navier-Stokes equation for incompressible stationary flow. A principal qualitative result of the analysis is the prediction (the reader is referred to the original papers for details)

$$1 - \frac{D_{11}(x,\eta)}{D_s(\eta)} \propto g_2(x-1) - 1 \quad (8)$$

with $D_s(\eta)$ the single particle self-diffusion coefficient at packing fraction η. This proportionality is exhibited by our data for a suspension in a bent q1D channel. The result is unexpected since, in the method of reflections calculation, transmission of the excess pressure generated by a displaced particle to the other particles includes a contribution from reflections at the boundary of the channel. For a straight channel these reflections are, at the level of approximation used, "one bounce," whereas in a bent channel we expect there to be at least a "two bounce" (and possibly "more bounce") contribution.

V. CONCLUSION

The confluence in a confined colloid suspension of the effects of direct particle-particle interactions with solvent mediated and transmitted hydrodynamic interactions leads to interesting questions when comparing systems with different geometries and boundary conditions. The constraint of single-file motion imposed on a colloid suspension by the geometry of a q1D channel requires examination of how hydrodynamic flow is affected by the bend in the channel, how colloid-colloid contact interactions are transmitted around the bend, and what coordinate system is most appropriate to describe the particle behavior. Focusing attention on Brownian motion in a q1D colloid suspension at equilibrium, we have used studies of the spatial correlation between a pair of particles in a bent q1D channel as a function of bend angle and of the pair diffusion tensor as a function of bend angle as the vehicle to address these questions. Noting that the boundary conditions that define the q1D channel require using the centerline of the channel as the coordinate onto which particle positions are projected, we observe a depletion of particles in the vicinity of the bend that increases as the angle becomes more acute, and an increase in the nearest-neighbor separation in the pair correlation function for particles on opposite sides of the bend as the angle becomes more acute.

We also observe that the peak value of $D_{12}(x)$, the coupling term in the pair diffusion tensor that characterizes the effect of the motion of particle 1 on particle 2, coincides with the first peak in the pair correlation function. This behavior of

$D_{12}(x)$ mimicking the pair correlation function is the same as that found experimentally and accounted for theoretically for colloid-colloid interaction in a straight q1D channel. We are then driven to the interesting and to us nonintuitive conclusion that under equilibrium conditions, in the absence of macroscopic flow, the hydrodynamic component of the colloid-colloid interaction is affected by the bend in the q1D channel only via the structural changes in the pair correlation function associated with the bend. For application to systems such as microchannel devices, further investigation will need to be performed to determine if these results hold in systems where the fluid has a substantial macroscopic velocity.

ACKNOWLEDGMENTS

We thank Bianxiao Cui for programming assistance, Robert Dellsy for help in fabrication of the channels, Peter Shin and Alex Lauro for early contributions to analysis of the experimental data, and John Marko for fruitful discussions. This work was supported by the NSF MRSEC (DMR-1420709) Laboratory at the University of Chicago and by a Grant from the Camille and Henry Dreyfus Foundation (Grant No. SI-14-014). B.L. acknowledges support from ChemMatCARS (NSF/CHE-1346572).

E.L. and R.Z. contributed equally as co-first authors to this work.

[1] J. C. Crocker, J. Chem. Phys. **106**, 2837 (1997).
[2] B. Cui, H. Diamant, and B. Lin, Phys. Rev. Lett. **89**, 188302 (2002).
[3] X. Xu, S. A. Rice, B. Lin, and H. Diamant, Phys. Rev. Lett. **95**, 158301 (2005).
[4] E. Kosheleva, B. Leahy, H. Diamant, B. Lin, and S. A. Rice, Phys. Rev. E **86**, 041402 (2012).
[5] K. Misiunas, S. Pagliara, E. Lauga, J. R. Lister, and U. F. Keyser, Phys. Rev. Lett. **115**, 038301 (2015).
[6] T. S. Davidsen, Numerical studies of flow in curved channels, Ph.D. thesis, University of Bergen, Norway, 2007.
[7] M. Falcon, Annu. Rev. Fluid Mech. **16**, 179 (1984).
[8] A. D. Dinsmore, A. G. Yodh, and D. J. Pine, Nature (London) **383**, 239 (1996).
[9] A. D. Dinsmore and A. G. Yodh, Langmuir **15**, 314 (1999).
[10] B. Cui, B. Lin, S. Sharma, and S. A. Rice, J. Chem. Phys. **116**, 3119 (2002).
[11] J. Crocker, J. Colloid Interface Sci. **179**, 298 (1996).
[12] S. L. Dettmer, S. Pagliara, K. Misiunas, and U. F. Keyser, Phys. Rev. E **89**, 062305 (2014).
[13] H. Diamant, J. Phys. Soc. Jpn. **78**, 1 (2009).
[14] J. B. Delfau, C. Coste, C. Even, and M. S. Jean, Phys. Rev. E **82**, 031201 (2010).
[15] Q.-H. Wei, C. Bechinger, and P. Leiderer, Science **287**, 625 (2000).